MedCrave
Step into the World of Research

Journal of Nanomedicine Research

Research Article

Open Access

CrossMark

Preparation and characterization of polyaniline/ZnO composite sensor

Abstract

Polyaniline/ZnO nanocomposite thin films were prepared via an electrochemical synthesis route on ITO coated glass substrates. ZnO nanoparticles were uniformly dispersed in to the polyaniline matrix. Interaction between ZnO nanoparticle and polyaniline has been studied using X-ray diffraction (XRD), UV-Vis absorption spectroscopy, PL spectroscopy, AFM and I-V characteristics. The ammonia gas sensing behaviors of the polyaniline/ZnO composites were examined at room temperature. It was observed that the composite films showed good sensitivity, improved doping state and enhanced photoluminescence behaviour.

Keywords: Polyaniline, ITO, AFM, UV-Vis absorption spectroscopy, Nanocomposites

Volume 5 Issue 1 - 2017

Akanksha Mehto,[1] Varsha R Mehto,[1] Jyotsana Chauhan,[2] Singh IB,[3] Pandey RK[1]

[1]Barkatullah University, India
[2]Rajiv Gandhi Proudyogiki Vishwavidyalaya, India
[3]Advanced Materials and Processes Research Institute, India

Correspondence: Jyotsana Chauhan, HOD in Nanotechnology, Rajiv Gandhi Proudyogiki Vishwavidyalaya, Bhopal, India Email jyotsnachauhan2006@gmail.com

Received: January 04, 2017 | **Published:** January 04, 2017

Abbreviations: SCE, Saturated Calomel; XRD, X-ray Diffraction; AFM, Atomic Force Microscopy

Introduction

Ammonia plays very crucial role for human health. The way of natural process in animals, human and plants are responsible for production of ammonia in atmosphere. High concentrations of ammonia can cause difficulty in breathing, irritation to the eyes and skin and long term exposure of NH_3 leads to fatal.[1] There is a variety of applications of artificially synthesized ammonia in chemical industry, fertilizer factories, textile, food processing, bleaching products and refrigeration systems.[2] Therefore the human activity is a main reason for the presence of larger amount of ammonia in our atmosphere and is a necessity to detect its presence. Hence much research has been focused on the development of suitable gas sensitive materials to detect lower concentration of NH_3 with excellent performance.[3]

There are several studies concerning metal oxides like SnO_2, WO_3, ZnO, TiO_2 for NH_3 sensing applications but generally it requires a high working temperature.[4,5] There are also several conducting polymers like polythiophene, polypyrrole and polyaniline are used for detecting gases, however, the poor selectivity is the main disadvantages of pure inorganic and organic materials. New and interesting properties can be achieved by combining organic and inorganic materials.[6] Therefore conducting polymer/inorganic nanocomposites are explored as promising materials for sensing application, because of their good ability and compatibility to form chemical sensors with higher sensitivity at room temperature.

Among the conducting polymers polyaniline based nanocomposites have many advantages. In literature, there are some reports available concerning the synthesis of polyaniline/metal oxide nanocomposites in gas sensing applications. Huyen et al.[7] synthesize polyaniline/TiO_2 nanocomposites and studies the effect of TiO_2 on the sensing features. Lee et al.[8] described the effects of O_2 plasma treatment on NH_3 sensing characteristics of multiwall carbon nanotube/polyaniline composite films. Wu et al.[9] reported the characterization and gas sensitivity study of polyaniline/SnO_2 hybrid material prepared by hydrothermal route. Deshpande et al.[10] reported tin oxide-intercalated polyaniline nanocomposite for ammonia gas sensing applications.

We employed simple electrochemical technique to synthesize polyaniline/ZnO nanocomposites. ZnO nanoparticles dispersed with the polyaniline chains enhanced the doping level and stability of composite structure due to the synergetic effect of the organic polymer and inorganic nanoparticles component, therefore polyaniline/ZnO composite is a promising material for the ammonia gas sensing application at room temperature. In this paper we discuss the ammonia sensing behaviour of polyaniline/ZnO composite structure with different weight percentage (wt %) of ZnO dispersed in polyaniline. The prepared composites were characterized by XRD, absorption and photoluminescence spectroscopy, atomic force microscopy and current voltage (I-V) characteristics.

Experimental techniques

Synthesis of ZnO nanoparticles

Chemical precipitation method was used for the synthesis of ZnO nanoparticles in a nonaqueous medium. In this synthesis 0.025M zinc acetate and 0.1M sodium hydroxide were added together at room temperature under continuous vigorous stirring. Precipitation was starts following few minutes. After 1 hour of stirring precipitation were collected using centrifugal machine and washed several times in ethanol and dried at room temperature.

Synthesis of polyaniline and polyailine/ZnO nanocomposites

Electrochemical synthesis of polyaniline was carried out using a potentiostat apparatus (EG&G, model 362, USA) with three electrode configuration cell. The three electrodes was working electrode, counter electrode and reference electrode. We used ITO coated glass plate as a working electrode, a platinum foil as the counter electrode, and a saturated calomel (SCE) as the reference electrode connected to the cell using a salt bridge. The electrode position bath contains 0.2M aniline and 0.3M HCl under continuous stirring at room temperature applying of constant DC potential of 1 V vs SCE. Finally the deposited film was rinsed several times with deionised water

Polyaniline/ZnO composites were also prepared by electrode position at a constant DC potential of 1 V vs SCE. In this synthesis different wt% of ZnO (with respect to aniline) nanoparticles were dispersed in an aqueous electrolyte solution containing 2:3 molar ratios of aniline and HCl. Three nanocomposite samples were

prepared using the different wt% of ZnO viz polyaniline/ZnO (2 wt%), polyaniline/ZnO (4 wt%) and polyaniline/ZnO (6 wt%).

Characterization techniques

X-ray diffraction (XRD) spectra were recorded by using the XRD (D8 Advanced Bruker, Germany) diffractometer, with CuKα radiation (1□542 Å). Optical absorption spectra of the ZnO nanoparticles and composite thin films were determined with the help of a UV-Vis spectrophotometer (UVPC 1601 Shimadzu, Japan). Fresh ITO substrate was used as a reference. Photoluminescence spectra of thin film samples were recorded from luminescence spectrophotometer (LS55 Perkin-Elmer Instruments, UK). Atomic force microscopy (Park System) was employed to examine the surface morphology. Cyclic voltammetry of the electrolytic solution and I-V characteristics of the composite films were examined with the help of an electrochemical analyzer (CH Instruments, model CHI 600E, USA).

Gas sensing test

In order to study the response of polyaniline and polyaniline/ZnO composite film to ammonia gas, aluminium contacts of 2 mm diameter were made on top of the film surface, by vacuum evaporation technique using vaccume coating unit. The chamber pressure during aluminium evaporation was kept around 0.5×10-6 Torr, and during metal evaporation, film substrates were not heated. A typical device structure for gas sensor has been shown in Figure 1A.

To test the ammonia gas sensitivity of polyaniline and composites films, the sensing electrode of composite thin film was placed in a lab-made U safe tube sensing system of 500 ml volume (Figure 1B). After reaches a steady-state, a certain amount of ammonia was injected into the test chamber. The changes in resistance of polyaniline and polyaniline/ZnO composite sensors were monitored and recorded by using a multimeter.

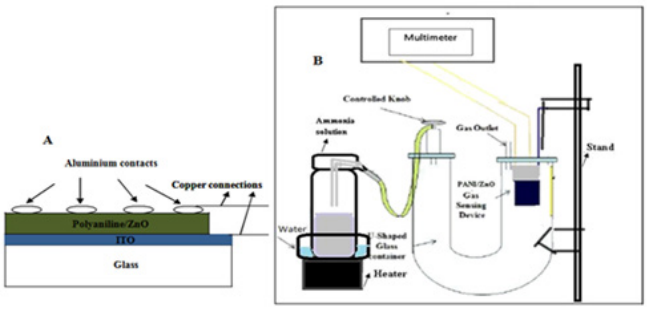

Figure 1 Schematic diagram of (A) polyaniline/ZnO composite sensing device and (B) sensitivity measurement system for ammonia gas.

During the measurements, different concentration of ammonia solution [25%] i.e.100, 200, 300, 400 and 500 ppm volumes were injected to the chamber. After the ammonia was introduced to the chamber, the resistance of the sensors was recorded for 600 s, then the test chamber was flushed with dry air consecutively for another 600 s to make sure that a relatively steady state had achieved before next cyclic test. The sensitivity (S) is defined as

$$S = \frac{(Ra - R0)}{R0}$$

Where Ra and R0 are the resistance of sensors in ammonia and in air atmosphere respectively.

Result and discussion

Cyclic voltammetry

The trend of growth of polyaniline film on working electrode was obtained using cyclic voltammetry. In the cyclic voltammetry study the particular onset of current or a peak reveals the occurrence of a specific electrochemical process. Sharma et al. reported that the electro polymerization of polyaniline, depending upon monomer concentration, pH, and the nature of the dopant.[11] Figure 2 shows a cyclic voltammogram of HCl doped polyaniline [0.2M aniline and 0.3M HCl] at a scan rate of 0.05 V/s. Weak noticeable peaks at -0.8, -0.11, and 0.6 V and a sharp exponential rise in anodic current at 1.0 V were recorded. Observed such weak peaks may be revealed the occurrence of various surface processes.[12,13] At the above potential, it is supposed that the aniline monomer undergoes a deprotonation/de-electronization reaction in this specified region as reported by Madhulika et al.[14] The peak at 1V was attributed to the emerldine salt form of HCl doped polyaniline. In reverse cycle of scan, we observed the two peaks at 0.13 and -0.48 V which corresponding to the reduction of polyaniline.

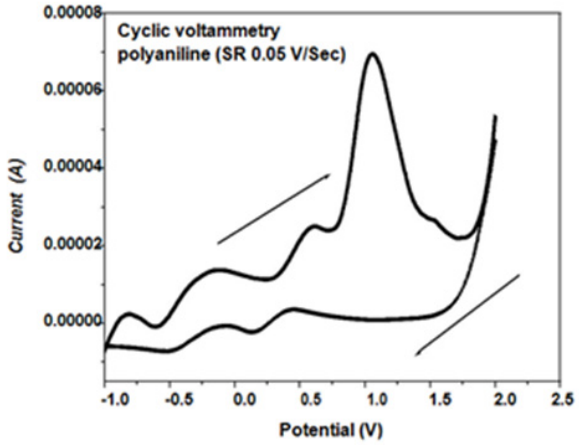

Figure 2 Cyclic voltammogram recorded for polyaniline doped with HCl on a platinum working electrode using a scan rate of 0.05V/sec in a solution containing 0.2M aniline and 0.3M HCl.

X-ray diffraction analysis

The XRD patterns obtained for ZnO and polyniline/ZnO nanocomposite are presented in Figure 3. The XRD pattern of ZnO Figure 3A shows broad peaks at 2θ = 32.80, 34.23, 35.92, 47.46, 59.44, 62.64 and 68.85 which corresponding to the (100), (002), (101), (102), (103), (200), and (104) plane of the hexagonal phase of ZnO respectively. These diffraction peaks show sharp and well defined peaks, indicate the good crystallinity of synthesize material.[15] The observed 2θ values are consistent with the standard JCPDS values. The crystallite size of nanoparticles was calculated using Scherrer's equation. The average size of the ZnO nanoparticles was found to be 7.5 nm.

The XRD pattern of polyaniline/ZnO composite (Figure 3B) contain the characteristic peaks of polyaniline and nanocrystalline ZnO. Diffraction peaks at 2θ= 15.16 , 20.46°, 23.35 and 25.24° are corresponding to the interplaner spacing of 5.73 Å, 4.33 Å, 3.81 Å and 3.53 Å respectively, which represent the emeraldine salt form of polyaniline.[14,16] The peaks at 2 =32.20 and 36.46 are corresponding to the nanocrystalline ZnO. The results indicated that ZnO crystallites have been uniformly mixed within the polymer chain. Notice that the

Citation: Mehto A, Mehto VR, Chauhan J, et al. Preparation and characterization of polyaniline/ZnO composite sensor. *J Nanomed Res.* 2017;5(1):1–6. DOI: 10.15406/jnmr.2017.05.00104

characteristic peaks of ZnO are slightly shifted, from their standard position in nanocomposites, which is due to the strong interaction between polyaniline and ZnO. Lee et al.[17] reported a similar peak shifting for polyaniline/SnO_2 composites. For all the samples, observed peak positions and d-spacing have been summarised in Table 1.

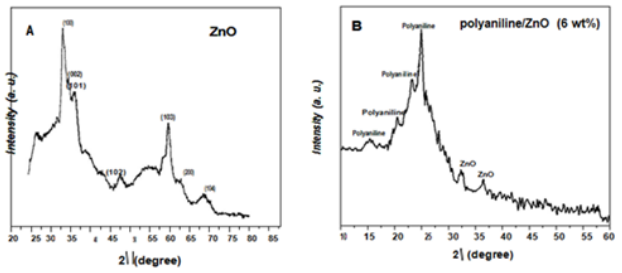

Figure 3 XRD spectra of ZnO, polyaniline and polyaniline/ZnO (6 wt% of ZnO) nanocomposites.

Table 1 Summary of XRD results: peak positions, d-values, phase assignments and the calculated particle size for the ZnO nanoparticles, polyaniline and polyaniline/ZnO (6 wt%) composite

Sample name	2θ (degree)	d-value (Å) Std.	Obs.	Phase assignment	Particle size of ZnO (nm)
	32.8	2.81	2.72	ZnO (Hexagonal)	
	34.23	2.6	2.61	ZnO (Hexagonal)	
	35.92	2.47	2.49	ZnO (Hexagonal)	
ZnO	47.46	1.91	1.91	ZnO (Hexagonal)	7.5
	59.44	1.55	1.55	ZnO (Hexagonal)	
	62.64	1.47	1.48	ZnO (Hexagonal)	
	68.85	1.37	1.36	ZnO (Hexagonal)	
	15.16	5.9	5.73	Polyaniline	
	20.46	4.4	4.33	Polyaniline	
	23.35	3.8	3.81	Polyaniline	
Polyaniline/ ZnO (6 wt %)	25.24	3.5	3.53	Polyaniline	≈7.5
	32.2	2.81	2.77	ZnO (Hexagonal)	
	36.46	2.47	2.46	ZnO (Hexagonal)	

Absorption measurements

The observed UV-Vis absorption spectra of ZnO, polyanilne and polyaniline/ZnO (2, 4 and 6 wt %) nanocomposites are shown in Figure 4.

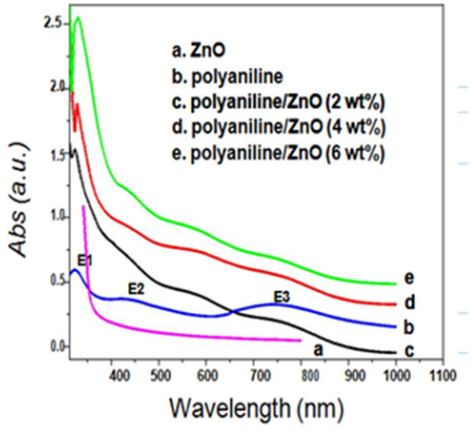

Figure 4 Optical absorbance spectra of (a) ZnO, (b) polyaniline, (c) polyaniline/ZnO (2 wt%), (d) polyaniline/ZnO (4 wt%) and (e) polyaniline/ZnO (6 wt%).

As shown in Figure 4 the sharp absorption onset at 350 nm is corresponding to the fundamental absorption edge of the ZnO nanoparticles. In the absorption spectra of polyaniline (Figure 4), the existence of three characteristic absorption bands around 322, 426 and 750 nm confirms the formation of doped polyaniline and comparable to the known spectral features of precisely characterized redox species of polyaniline.[18] The absorption band at 322 nm is due to the π-π* transition within the benzonoid segment. The second absorption band at 426 nm is attributed to the doping level of polyaniline (polaron-π* transition) and the absorption band at 750 nm is related to the formation of localized polaron at the backbone of the polymer (π-polaron transition).[19-21] The absorption band positions and corresponding intensities have been reported in Table 2.

Table 2 Observed absorption peak positions and the normalized intensities for ZnO nanoparticles, Polyaniline and Polyaniline/ZnO composites thin films

Sample	Absorption Peak Position (nm)			Intensity (Normalized)	
	E1	E2	E3	E1/E2	E1 /E3
Polyaniline	322	426	750	130	121
polyaniline/ZnO (2 wt%)	323	430	756	215	200
polyaniline/ZnO (4 wt%)	328	433	762	201	346
polyaniline/ZnO (6 wt%)	330	439	770	212	392

From the absorption spectra of composites (Figure 4), we can see that the absorption band due to π-π* transition in the nanocomposites exhibit a increasing red shift from polyaniline to polyaniline/ZnO (6 wt%). Moreover the relative intensities of these bands increase in the composite structures. The observed red shift in the absorption bands may be due to the increasing wt% of ZnO nanoparticles and their interaction with polyaniline.[22] Similarly, a systematic red shift was also observed in the peak position for the polaron- π* and π-polaron absorption band in the nanocomposite samples. However, the comparative intensity of these bands decreased remarkably with the increase wt% of ZnO. The intensity of polaron absorption band was decreased with higher doping level due to the uniform distribution of radical cation at the backbone of polymer.[23] The decreasing intensity of π-polaron absorption band at ≈750 nm indicated that the doping state improved by ZnO dispersion.

Photo luminescence measurements

Figure 5A represents the photoluminescence spectra of ZnO nanoparticles using excitation wavelength of 300 nm. ZnO exhibited PL peaks at 384 nm, 422 nm and 553 nm. The observed peak at 384 nm is close to the absorption edge of ZnO observed at 350 nm. The observed slight red shift in the PL emission peak from the fundamental absorption edge may be assigned to the electron-phonon or Frohlich interactions.[24] The strong green emission band at ~553 nm is due to the defects on the surfaces of nanoparitcles. It is reported that the green emission of the ZnO nanoparticles results from the surface defects formed by oxygen vacancies or the zinc interstitials on the ZnO nanoparticles surface.[25,26]

The PL spectra of polyaniline and polyaniline/ZnO nanocomposite [2,4 and 6 wt% of ZnO] using the excitation wavelength of 300 nm are given in Figure 5B. Polyaniline shows the luminescence peak at 380 nm (Figure 5B), which is due to the recombination involving the polaron bands have been reported in the literature.[27] The luminescence peak positions, corresponding FWHM and the normalized intensities observed by PL spectra also reported in Table 3.

Citation: Mehto A, Mehto VR, Chauhan J, et al. Preparation and characterization of polyaniline/ZnO composite sensor. *J Nanomed Res.* 2017;5(1):1–6. DOI: 10.15406/jnmr.2017.05.00104

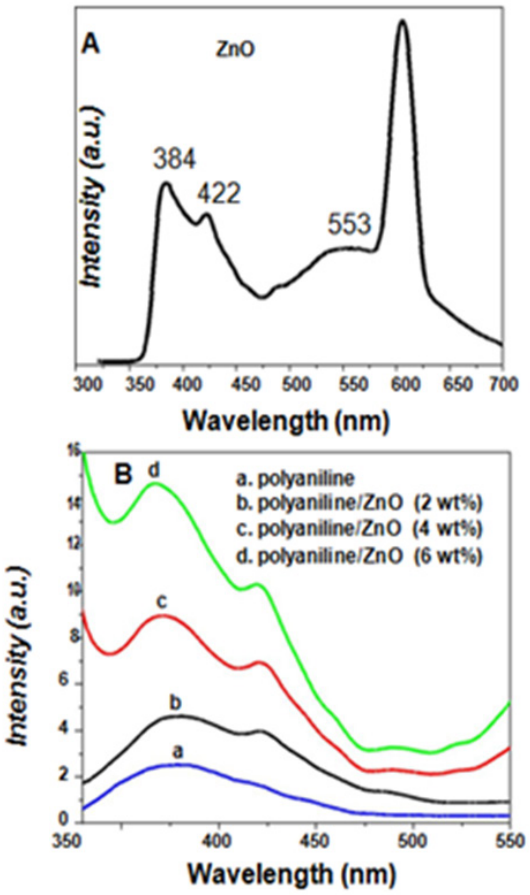

Figure 5 [A] PL spectra of ZnO nanoparticles, [B] PL spectra of polyaniline and polyaniline/ZnO composites using 2, 4 and 6 wt% of ZnO [Ex. wavelength 300 nm].

Table 3 The observed peak positions, corresponding FWHM and the normalized intensities in the PL spectra of ZnO, polyaniline and polyaniline/ZnO composites

Sample	Peak (nm)	Positions FWHM (nm)	Normalized Intensity
ZnO	378	51	-
Polyaniline	380	70	17.06
Polyaniline /ZnO (2 wt%)	378	81	31.3
Polyaniline/ZnO (4 wt%)	370	34.2	61
Polyaniline/ZnO (6 wt%)	368	25.6	100

In Figure 5B-D the nanocomposite samples polyaniline/ZnO [2, 4, 6 wt%] composites also shows the luminescence spectra similar to the corresponding ZnO nanoparticle dispersants but with a considerable enhancement in the relative band edge luminescence intensity with increasing weight persent of ZnO. The enhancement in PL intensity may be related to the process of charge transformation between the electronic levels of polyaniline and ZnO. Due to the strong interaction the charge transfer increases thus the enhancement in PL intensity was observed similar type results have been reported by Weng et al.[28] for PEO/CdS/polyaniline composite. Further it is observed that as the concentration of ZnO increased in polyaniline, the band edge luminescence peak was slightly blue shifted. The observed blue shift may also be due to the strong interaction between polyaniline and ZnO nanoparticles.[29]

Morphological characterization

To study the surface morphology of polyaniline and composite films atomic force microscopy was employed. Figure 6A shows the AFM micrograph of the HCl doped polyaniline which represents the dense packing of ordered polymer bundles. Madhulika et al.[14] also reported similar type of dense packing of ordered polymer bundles in HCl doped polyaniline films.

The AFM morphology of polyaniline/ZnO (2 wt%), polyaniline/ZnO (4 wt%) and PANI/ZnO (6 wt%) are shown in Figure 6 B-D respectively. A flower like features is observed in composite sample with 4 and 6 wt% of ZnO loading. Moreover, we observed that higher loading of ZnO (6 wt%) in the polyaniline host lead to increase in the size of the polymeric flower like bundles. The differences in the surface morphology are due to the strong interaction between the nanoparticles and the polymer due to different loading of ZnO. A typical high resolution AFM images of sample polyaniline/ZnO (6 wt%) is also shown in Figure 6E & 6F.

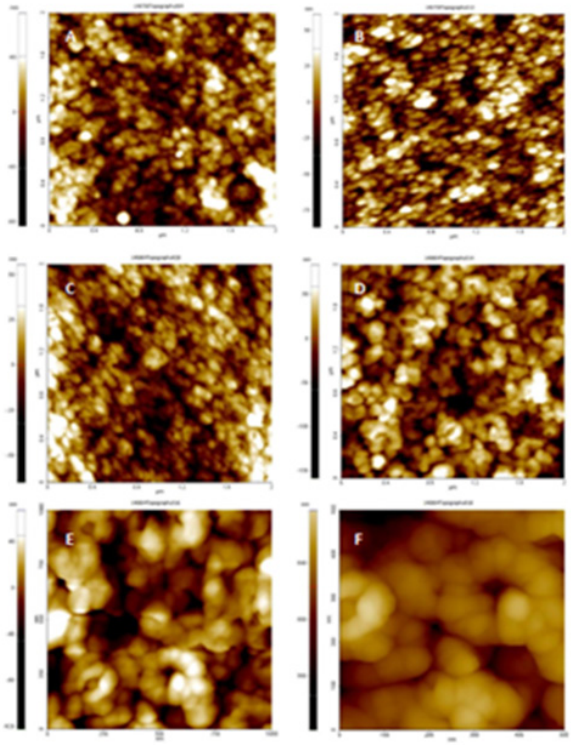

Figure 6 The observed two dimensional AFM images of (A) polyaniline, (B) polyaniline/ZnO (2 wt%), (C) polyaniline/ZnO (4 wt%) and (D) polyaniline/ZnO (6 wt%) thin films. (E) and (F) corresponding to high resolution image of sample polyaniline/ZnO (6 wt%).

I-V curve of polyaniline and polyaniline/ZnO nanocomposite using 2, 4 and 6 wt% of ZnO are shown in Figure 7. All these curves show apparently rectifying behaviour and the current is continuously increased with applied voltage. However in the case of polyaniline/ZnO nanocomposites the current values is much higher as compared to pure polyaniline. Further we can see that as the weight percent of ZnO in polyaniline host increases then the current is also increase therefore these curve indicated that the highest values of current at the higher concentration of ZnO. The turn on voltage for HCl doped polyaniline, polyaniline/ZnO (2 wt%), polyaniline/ZnO (4 wt%) and polyaniline/ZnO (6 wt%) were recorded are 0.38, 0.45, 0.70, and 0.85V respectively.

Citation: Mehto A, Mehto VR, Chauhan J, et al. Preparation and characterization of polyaniline/ZnO composite sensor. *J Nanomed Res.* 2017;5(1):1–6.
DOI: 10.15406/jnmr.2017.05.00104

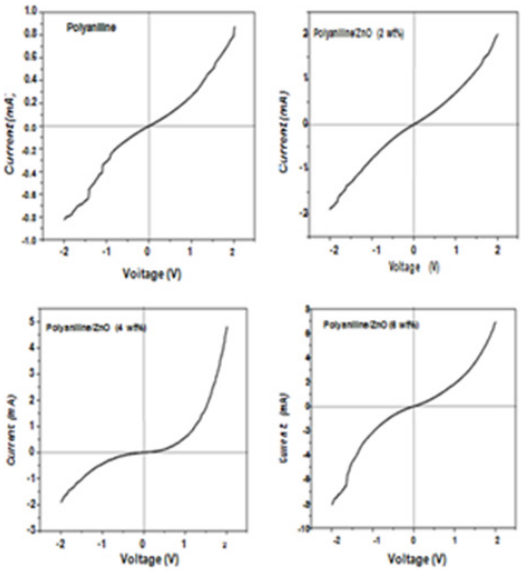

Figure 7 I-V characteristics of polyaniline and polyaniline/ZnO composites using 2, 4 and 6 wt% of ZnO.

Gas sensing analysis

The ammonia sensing profile of polyaniline, polyaniline/ZnO (2 wt%), polyaniline/ZnO (4 wt%) and polyaniline/ZnO (6 wt%) nanocomposites have been shown in Figure 8. The resistance of polyaniline and all the three polyaniline/ZnO composite sensing devices were increased as ammonia gas is injected. The gas sensitivity percentage of all the samples was observed to increase continuously with increasing the gas concentration in the range 100- 500 ppm.

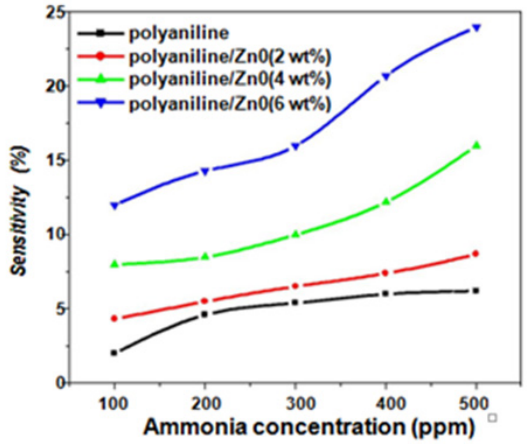

Figure 8 Ammonia sensitivity of polyaniline and polyaniline/ZnO (2 wt%), polyaniline/ZnO (4 wt%) and polyaniline/ZnO (6 wt%) composites for different concentration of ammonia.

In the case of polyaniline alone the sensitivity is low due to lower adsorption of ammonia molecules because of lower surface area. Further it is also observed that the sensitivity is strongly depending on wt% of ZnO. The sensitivity of polyaniline/ZnO composites was found to be increased as the wt% of ZnO in polyaniline increased. The highest sensitivity percent is found in the nanocomposite containing 6 wt% of ZnO. Since we know that HCl doped polyaniline thin film is normally a p type semiconductor while ZnO is a n type semiconductor. In presence of ZnO crystallites, the polyaniline matrix gets a modified structure electronically therefore a p-n junction formed.[30] The appearance of a variety of p-n semiconductor contacts likely facilitates the formation of various gas molecular adsorption sites on the polyaniline surface thus the sensitivity is increased as compare to pure polyaniline.[7] The electrical conductivity of polyaniline/ZnO composites was found to be much higher then polyaniline and increased with increasing ZnO concentration in polyaniline matrix. Thus the highest sensitivity was found in the composite sample with higher loading of ZnO.

We also studied response and recovery time of the films with respect to ammonia gas exposure. The response time, and the recovery time are defined as the time required for a film resistance to reach 90% of its saturation value from the starting value on gas exposure, and on removal of the gas, respectively. In our case, the polyaniline films had relatively faster response times 10 sec at ammonia concentration of 300 ppm, but as usual the recovery times were relatively larger, around 550 sec. The larger recovery times are likely due to the slow rate of diffusion. The polyaniline/ZnO nanocomposites films have response times of 10-30 sec, and the slower recovery times as compare to polyaniline. Recovery time for polyaniline/ZnO nanocomposite was increased with increasing wt% of ZnO it was ~ 20 min for polyaniline/ZnO (6 wt%) at ammonia concentration of 300 ppm.

Conclusion

We have presented the successful fabrication of polyaniline and polyaniline/ZnO nanocomposites for ammonia gas sensing application. Different weight percent of ZnO have been uniformly dispersed into the polyaniline matrix. The resulting composites were characterized by X-ray diffraction, optical absorption spectroscopy, luminescence spectroscopy, atomic force microscopy, I-V characteristics and sensitivity measurement study. XRD studies confirmed the dispersion of ZnO nanoparticles in polyaniline matrix. The lower intensity polaron absorption bands for polyaniline/ZnO nanocomposites in the UV-Vis spectra indicate that the conducting state of the polymer has been improved. Observed results clearly indicate that polyaniline/ZnO nanocomposite is a good candidate for ammonia sensing with better sensitivity. Photoluminescence measurements represent the improvements in the photoemission following dispersion. I-V characteristics revealed that polyaniline/ZnO sensing device shows more current response as the weight percent of ZnO is increased in polyanilne host, therefore the highest values of current at the higher concentration of ZnO. Sensitivity measurements revealed that the resistance of polyaniline/ZnO composite sensing devices increases with the injection of ammonia gas. The highest sensitivity was found in the composite sample with higher loading of ZnO.

Acknowledgments

None.

Conflicts of interest

None.

References

1. Timmer B, Olthuis W, Den Berg AV. Ammonia sensors and their applications–a review. *Sensors and Actuators B*. 2005;107(2):666–677.
2. Wrenn C. Real time measurement of ammonia gas. *Occupational Health and Safety*. 2000;69(12):64–67.
3. Qingqing Wang, Xianjun Dong, Zengyuan Pang, et al. Ammonia sensing behaviors of TiO_2–PANI/PA6 composite nanofibers. Sensors. 2012;12(12):17046–17057.

4. Hieu NV, Quang VV, Hoa ND, et al. Preparing large–scale WO_3 nanowire–like structure for high sensitivity NH_3 gas sensor through a simple route. *Current Applied Physics*. 2010;11:657–661.
5. Sánchez M, Rincón ME. Sensor response of sol–gel multi walled carbon nanotubes–TiO_2 composites deposited by screen–printing and dip–coating techniques. *Sensors and Actuators B*. 2009;140(1):17–23.
6. SJ Su, N Kuramoto. Processable polyaniline–titanium dioxide nanocomposites, effect of titanium dioxide on the conductivity. *Synth Met*. 2000;114(2):147–153.
7. Duong Ngoc Huyen, Nguyen Trong Tung, Nguyen Duc Thien, et al. Effect of TiO_2 on the gas sensing features of TiO_2/PANi nanocomposites. *Sensors*. 2011;11(2):1924–1931.
8. Yoo KP, Kwon KH, Min NK, et al. Effects of O_2 plasma treatment on NH3 sensing characteristics of multiwall carbon nanotube/polyaniline composite films. *Sensors and Actuators B: Chemical*. 2009;143(1):333–340.
9. L Geng, Y Zhao, X Huang, et al. Characterization and gas sensitivity study of polyaniline/SnO_2 hybrid material prepared by hydrothermal route. *Sens Actuators B*. 2007;120:568–572.
10. Sharma SK, Sharma AB, Sharma M, et al. Structural and optical investigation of semiconductor CdSe/CdS core–shell quantum dot thin films. *J Nanoengineering and Nanosystem*. 2009;72(2):285–290.
11. Maboudian R. Surface processes in MEMS Technology. *Surf Sci Rep*. 1998;30(6–8):207–269.
12. Winters HF, Coburn JW. Surface science aspects of etching reactions. *Surface Science Reports.* 1983;14(4–6):162–269.
13. Madhulika Sharma, Diksha Kaushik, Ragini R Singh, et al. Study of Electropolymerised Polyaniline Films Using Cyclic Voltammetry, Atomic Force Microscopy and Optical Spectroscopy. *J Materials Science–Materials in Electronics*. 2006;17(7):537–541.
14. Ahmed F, Kumar S, Arshi N, et al. Preparation and characterizations of polyaniline (PANI)/ZnO nanocomposites film using solution casting method. *Thin Solid Films*. 2011;519(23):8375–8378.
15. Buron CC, B Lakard, Monnin AF, et al. Elaboration and characterization of polyaniline films electrodeposited on tin oxides. *Synthetic Metals*. 2011;161(19–20):2162–2169.
16. Deshpande NG, Gudage YG, Sharma R, et al. Studies on tin oxide–intercalated polyaniline nanocomposites for ammonia gas sensing applications. *Sensors and Actuators B*. 2009;138(1):76–84.
17. Wessling B. Scientific and Commercial Breakthrough for Organic Metals. *Synth Met*. 1997;85(1–3):1313–1318.
18. Y He. A novel emulsion route to sub–micrometer polyaniline/nano–ZnO composite fibers. *Appl Surface Sci*. 2005;249:1–6.
19. HC Pant, MK Patra, SC Negi, et al. Studies on conductivity and dielectric properties of polyaniline–zinc sulphide composites. *Bulletin of Materials Science*. 2006;29(4):379–384.
20. Sarma TK, A Chattopadhyay. Reversible encapsulation of nanometer–size polyaniline and polyaniline–Au–nanoparticle composite in starch. *Langmuir*. 2004;20(11):4733–4737.
21. Khanna PK, SP Lonkar, VVVS Subbarao, et al. Polyaniline–CdS nanocomposite from organometallic cadmium precursor. *Materials Chemistry and Physics*. 2004;87(1):49–52.
22. Han MG, SK Cho, SG Oh, et al. Preparation and characterization of polyaniline nanoparticles synthesized from DBSA micellar solution. *Synth Met*. 2002;126(1):53–60.
23. J Mazher, S Badwe R Sengar, Gupta D, et al. Strained ZnSe Nanostructures Investigated by XRD, AFM, TEM and Optical Spectroscopy. *Physica E*. 2003;16:209.
24. Ahn Cheol Hyoun, Kim Young Yi, Kim Dong Chan, et al. A comparative analysis of deep level emission in ZnO layers deposited by various methods. *Journal of Applied Physics*. 2009;105(1):013502.
25. Borgohain K, Mahamuni S. Luminescence behaviour of chemically grown ZnO quantum dots. *Semiconductor Science and Technology*. 1998;13(10):1154–1157.
26. Strafstrom S, JL Bredas, AJ Epstein, et al. Polaron lattice in highly conducting polyaniline: Theoretical and optical studies. *Phys Rev Lett*. 1987;59:1464.
27. G Yu, X Li, X Cai, et al. The photoluminescence enhancement of electrospun poly(ethylene oxide) fibers with CdS and polyaniline inoculations. *Acta Materialia*. 2008;56(19):5775–5782.
28. Varsha R Mehto, Deepshikha Rathore, RK Pandey. Optical and structural properties of electrodeposited polyaniline/Q–CdS composite. *Polymer Composites*. 2014;35(9):1864–1874.
29. Kukla AL, Shirshov YM, Piletsky SA. Ammonia sensors based on sensitive polyaniline films. *Sens Actuat B*. 1996;37(3):135–140.
30. Xing Jiu Huang, Yang Kyu Choi. Chemical sensors based on nanostructured materials. *Sensors and Actuators B*. 2007;122:659–671.